*ICOLD Symposium on Sustainable Development of Dams and River Basins, 24th - 27th February, 2021, New Delhi*

# CAHORA BASSA DAM. STOPLOG OPERATION AND REGULATING GATES INSTRUMENTATION

**J.F. MELO**
*National Laboratory of Civil Engineering, Lisbon, Portugal*

**E.F. CARVALHO AND C. MALAUENE**
*Hidroeléctrica de Cahora Bassa, Songo, Mozambique*

**I. MEIRELES**
*Aveiro University, Aveiro, Portugal*

**P. PINOTES**
*LTu Engenharia, Lisbon, Portugal*

## ABSTRACT

*The Mozambican Cahora Bassa 171 m high concrete arch dam in the Zambezi River operated by HCB since 1977 has a spillway with 14 000 m$^3$/s capacity, comprising eight identical high-head orifices (8x1680 m$^3$/s) in the dam body. Dam observation and monitoring evidenced an alkali-aggregate reaction process that is inducing deformations on the dam body affecting the geometry of the rectangular spillway orifices. This process leads to an increased risk of blockage during gate maneuvers. In case of blockage, the upstream stoplog has to be lowered under full head (85 m) to cut the flow. As this emergency operation poses some concern to the dam operator, hydraulic model studies involving a 1/40 physical model complemented with numerical CFD simulations were carried out to assess the hydraulic operation conditions of the upstream stoplog. Pressure fluctuations and downpull force were experimentally characterized. Flow patterns were numerically assessed. Conditions and limitations for a safe stoplog operation were then assessed. The radial gates were subject to deep rehabilitation works and instrumentation was installed allowing remote real-time monitoring of operating effort and loads on the strut arms, trunnions and side guide rollers. Hydraulic models and gates' instrumentation will be described in the paper.*

## 1. INTRODUCTION

The Cahora Bassa arch dam is located on the Zambezi River in the Tete Province of North-Western Mozambique. Commissioned in the 1970's, the dam is mainly intended for hydro power production, but also manages the hydrology of a lake 270 km long and 35 km wide, with maximum capacity of 65,000 hm$^3$. It is a 171 m high double curvature concrete arch on granite rock foundation. It incorporates eight mid-level spillways with discharge capacity of 13,440 m$^3$/s and one surface spillway at the crest axis with maximum discharge of 550 m$^3$/s. The eight mid-level spillways are symmetrically positioned towards the center of the dam (Fig. 1). Mid-level orifices are identical, presenting constant 6 m width and a convergent/ascending profile with 15 m height at upstream section and 7.8 m at downstream section. A radial regulating gate is placed downstream and an exit lip with 32.5° with horizontal maximizes the jet's reach. Protruding structures on the upstream dam face enhance flow conditions into the orifices and allow the placement of a stop-log.

The eight mid-level spillway gates, besides allowing the control of flood discharges, also allow the management of the reservoir as set in the Dam Water Level Curve Guide, so that in pre-defined periods of year, the water is conveyed downstream through the spillway to reduce the reservoir water level before the rainy season. The radial spillway gates operate under high heads (85 m) and velocities (40 m/s), being their water tightness in closed position a key functional aspect to be ensured.

Regulating gates are materialized by a 13.5 m radius curved skin-plate, a frame with rubber seals that provide water-tightness and two lateral guide rollers on each side. The gate leaf is connected to two trunnion pins with two lattice type arms. Both trunnion pins are fixed to a reinforced concrete horizontal beam, connected to two reinforced concrete consoles overhanging the dam.

Each radial gate is operated by a centrally positioned servomotor, connected to the gate leaf with a suspension bar. During movement, the gates are guided between fixed stainless-steel side embedded parts. In the lower section, these embedded parts are integrated with the 20 mm plate of the steel lined orifice, ensuring gate guiding and water-tightness functions. In the upper section, above the sluice opening, the embedded parts only consist of thin plates, welded on a support, anchored in concrete, ensuring contact of rubber seals and side guide rollers when the gate is opened (Fig. 2).

**Figure 1** : Cahora Bassa dam.

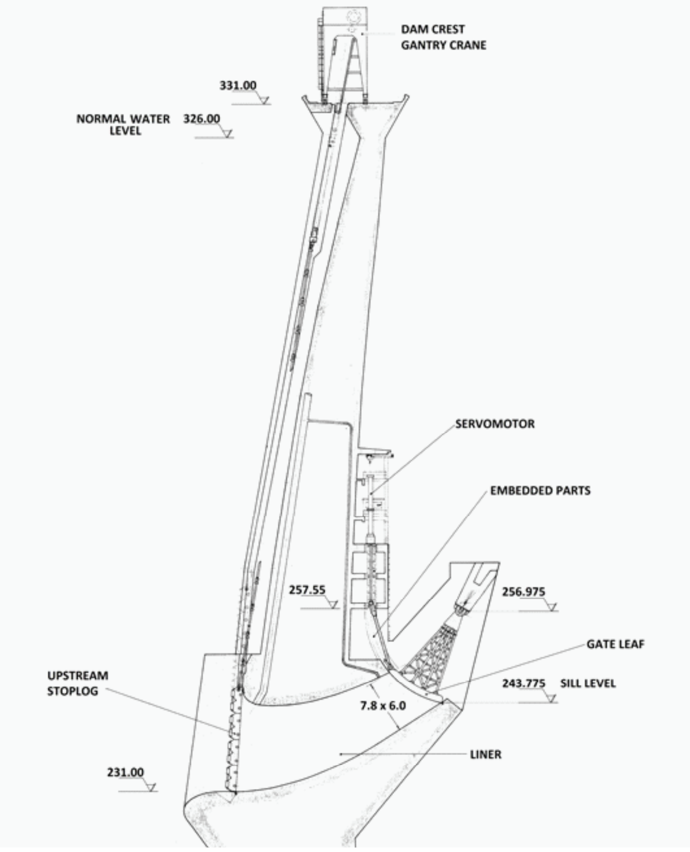

**Figure 2** : Cross-section view of the dam.

The main radial gates particularities that increase difficulties in inspection operations and works are:

- The large gates dimensions (6.0 m wide x 7.8 m high), the cantilever position on the dam downstream face and the high sloping positions (60° angle versus horizontal);
- Functionality at all times involve close compliance to geometrical and dimensional tolerances.

Each mid-level spillway can be dewatered by lowering a stoplog (bowstring caterpillar type gate) down the upstream face of the dam, guided by side slots and suspended from a rolling gantry crane on the dam crest (load capacity of 3,920 kN). The stoplog, formed by four similar 3.80 m high and 7.57 m wide elements (Fig. 3), has a total height of 15.20 m and weighs 1,512 kN. The stoplog upper seal is mounted at the top of the upper element downstream face and works against de orifice sill beam. Side seals work along the downstream face of the gate slot and continuously link to the bottom seal at the gate lip. The suspension bar assembly for the gate maneuver weighs 195 kN.

**Figure 3** : Downstream face of one of the four elements of the stoplog (the photo is distorted).

In the scope of the dam observation, monitoring and maintenance, evidences of developing alkali-aggregate reaction process were detected. The resulting deformations on the dam body have been progressively affecting the geometries of the spillway orifices, posing problems to the reliability of the spillway regulating gates maneuvers and, therefore, to the dam safety. HCB initiated a program involving the safety studies to cope with scenarios of a gate blockage as well as the spillway and gates rehabilitation and improvement of gate surveillance and monitoring (Botha et al. 2016).

## 2. HYDRAULIC MODEL STUDIES OF STOPLOG OPERATION

Model studies were performed based on physical (LNEC, 2019) and numerical (UA, 2018) approaches to analyze the stoplog hydraulic operation under full flow conditions, assuming undesired regulating gate blockage in partially or fully opened positions, as described in the next sections.

### 2.1 Physical model

A physical model was conceived in order to allow steady-state tests, for pre-defined stoplog and regulating gate opening combinations, meant to determine the most unfavorable hydraulic operating conditions, and unsteady state tests, under full head for five assumed preset blocked positions of the regulating gate (100%, 80%, 60%, 40% and 20%), meant to determine downpull force curves in the stoplog suspension chain.

The physical model, explored based on Froude similarity, comprised a 1/40 scale reproduction of one of the eight mid-level orifices. The metal tank built to simulate the reservoir hydraulic boundary conditions (Fig. 4, left) allowed the reproduction of 120 m of upstream extension (3 m in the model), 50 m for each side of the orifice symmetry axis (1.25 m in the model) und maximum head of 85 m (2.1 m in the model). Transparent material was used to reproduce the mid-level orifice in order to allow flow visualization. The aeration devices were duly reproduced, despite the unavoidable scale effects. Thirteen piezometric pressure taps were provided on the ceiling axis and another nine on the left side wall of the orifice. Also, four pressure transducers were mounted on the left side wall and one on the bottom sill below the stoplog working plane.

The model of the stoplog was conceived so that the flow and its hydrodynamic effects on the gate would be properly reproduced in order to properly assess the downpull force. The stoplog was materialized by means of 3D printing, ABS having been the chosen material (Fig. 4, right). Additional reinforcement was introduced in stoplog adding brass structural elements. The gate seals were approximately reproduced by imposing a nominal 0.1 mm spacing between the stoplog downstream face and the gate slots and orifice sill beam. The prototype tracks were replaced in the model by four steal rolling bearings placed on each side of the gate. A linear motion actuator equipped with a position sensor and a load cell was used to reproduce and control the stoplog movements and record the downpull force throughout the movement. The model regulating gate was made using brass.

**Figure 4** : Physical model. General view on the left and stoplog model (upstream face) on the right.

## 2.2 Numerical model

For the numerical, which only concerned the flow characterization of steady state simulations, the *FLOW-3D®* software was used. It solves the fluid equations of motion combining the discretization methods of finite differences and finite volumes in a Cartesian grid. The considered governing flow equations are:

$$\frac{\partial\overline{u_i}}{\partial x_i}=0 \tag{1}$$

$$\mathrm{r}_0\left[\frac{\partial\overline{u_i}}{\partial t}+\frac{\partial\left(\overline{u_i}\,\overline{u_j}\right)}{\partial x_j}\right]=\mathrm{r}_0 g_i+\mathrm{m}\frac{\partial^2\overline{u_i}}{\partial x_j^{\,2}}-\frac{\partial\overline{p}}{\partial x_i}-\frac{\partial\overline{u_i'u_j'}}{\partial x_j} \tag{2}$$

where $\overline{u_i}$ and $\overline{u_j}$ are the time–averaged velocity components in the directions $x_i$ and $x_j$; $r_0$ is the reference density; $t$ is the time coordinate; $g_i$ is the component of the acceleration of gravity in the direction $x_i$; m is the dynamic viscosity; $\overline{p}$ is the time–averaged, modified pressure; and $u_i'$ and $u_j'$ are the fluctuating velocity components in the directions $x_i$ and $x_i$. $-\mathrm{r}\,\overline{u_i'u_j'}$ represents the momentum transport due to turbulent motion, acting as fluid additional stresses (Reynolds stresses). Turbulence was modelled considering the Boussinesq approach and taking into account the standard *k - e* turbulence model (Launder & Spalding, 1972).

The domain where the governing equations are valid is composed by part of the reservoir, the spillway orifice and a portion of the downstream area. To locate the free surface, *FLOW-3D®* uses the *TruVOF* method (Hirt & Nichols, 1981). The following boundary conditions were also considered: (i) water level in the reservoir; (ii) downstream water level; and (iii) rigid wall at the bottom of the entire domain. Null normal velocity at the solid surface and the usual wall functions to take turbulence close to the walls into account were imposed (Pope, 2000; Ferziger & Peric, 2002).

The geometry was defined in a CAD file, based on the dimensions of the dam and the mid-level spillway orifice and subsequently imported into *FLOW-3D®* in STL format. In order to get compatible object resolution, computer memory and calculation time, a detailed study was performed for different meshes considering: (i) a full 3D model; (ii) a 3D model considering a symmetry plan; (iii) a pseudo 2D model, one meter wide (Fig. 5). The herein presented results were obtained using the model of situation (iii), for which several simulations considering increasingly higher mesh resolutions were performed until no significant results improvement was observed (total of 2.1x$10^5$ cells).

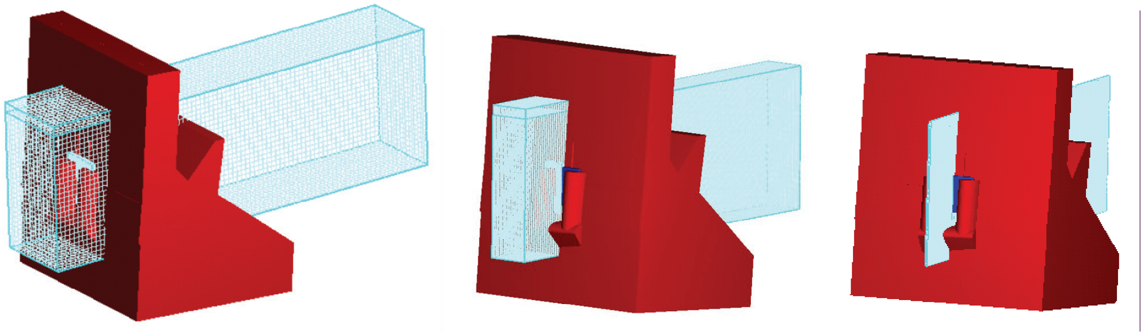

**Figure 5** : Improvements and simplifications of the numerical model used meshes and domains (UA, 2018).

## 2.3 Hydraulic Models' Results

### 2.3.1 *Steady state simulations*

For each preset regulating gate blocked position, the most severe stoplog position was obtained by continuously observing the evolution of the pressure in the orifice ceiling piezometric taps while the stoplog was slowly lowered (Tab. 2).

**Table 2** : Opening combinations for stoplog and regulating gate

| Stoplog opening (%) | Regulating gate blocked position (%) |
|---|---|
| 76 | 100 |
| 51 | 80 |
| 35 | 60 |
| 19 | 40 |
| 6 | 20 |

The stoplog most severe positions in Table 2 were empirically assessed as being those leading to minimum values of the pressure on the orifice ceiling. It corresponds to the lowest position of the stoplog before air starts being aspired through the air vents (Fig. 6).

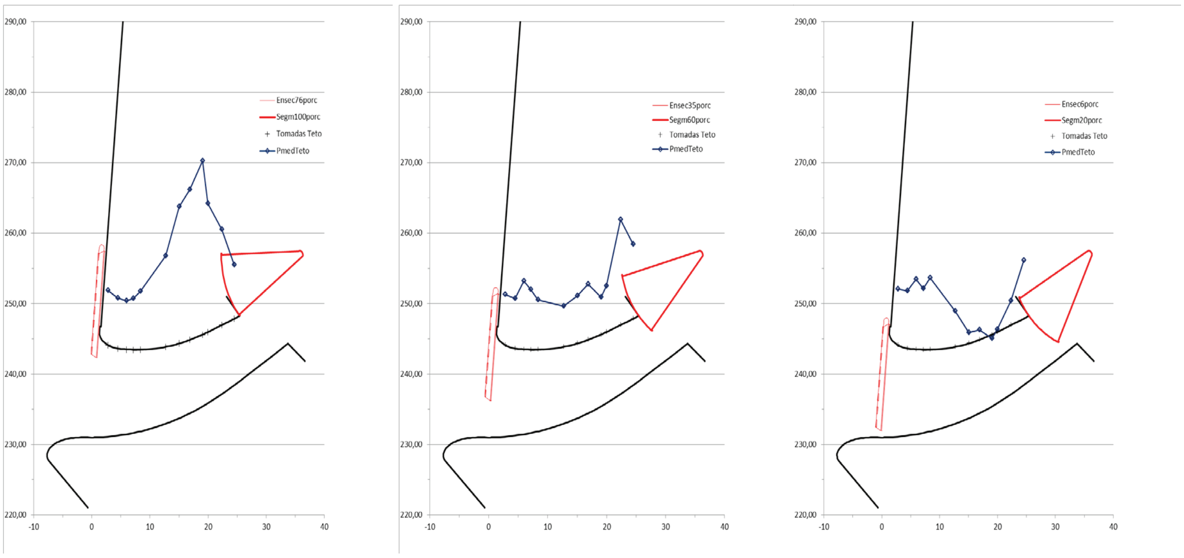

**Figure 6** : Mean piezometric pressures on the ceiling pressure taps (regulating gate 100%,60% and 20%) .

Considering that the flow in the orifice during the stoplog maneuver presents, for some opening combinations, an intensely disturbed and pulsatory character, to which very relevant pressure fluctuations are associated, the determination of the worse position was inevitably empiric. Particularly useful for this procedure was the possibility of directly observing the flow in the orifice fully transparent walls.

The results indicate that the most severe pressure fluctuations occur in a wider range of cofferdam positions when blocking of the regulating gate occurs between the 20% and 80% openings. Within this range of possible regulating gate blocking positions, it was also found that between openings of 40% and 60% the most severe pressure fluctuations amplitudes occur. The flow disturbances in the orifice are reflected in the jet flow patterns, as it is evidenced in Figure 7, in which the jet produced under normal operation (no stoplog) is compared against the jet produced under stoplog operation. This situation is due to disturbances generated in the velocity, pressure and turbulent fields by the presence of the stoplog cutting the flow as it becomes evident from the patterns of these fields shown in the graphs of Figure 8, from the numerical model.

**Figure 7** : Jet flow patterns under normal operation (above) and during the stoplog maneuver (bottom).

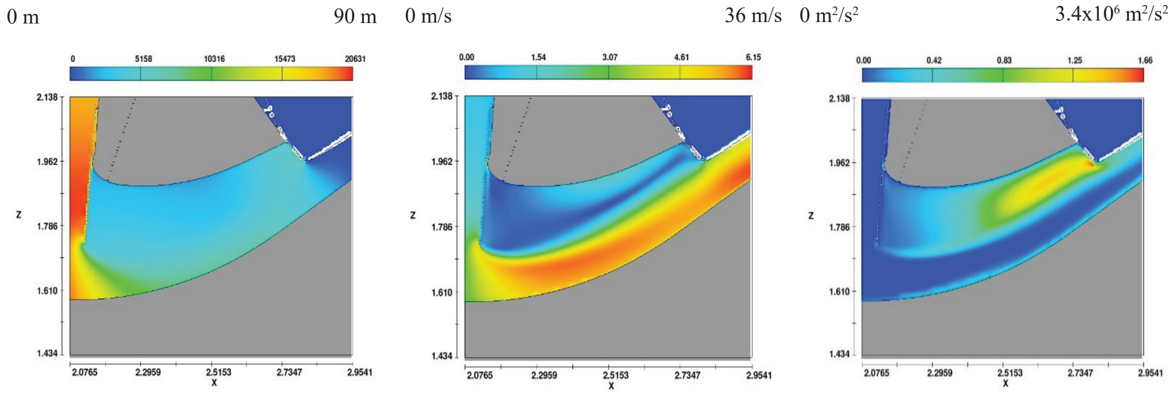

**Figure 8** : Numerical model. Pressure, velocity and turbulent fields (stoplog 40% and regulating gate 60%).

Recordings of pressure fluctuations, which mostly result from pulsating mass oscillations, as detected by the in-phase values at all measurement points in the orifice, indicate that within the range of blocked regulating gate positions between 40% to 60%, a maximum pressure fluctuation amplitude of 22 m of water column is produced, *i.e.*, 26% of the 85 m head imposed by the upstream reservoir. For the blocked regulating gate positions of 20% and 80% the maximum pressure amplitudes drop, respectively, to 10 and 14 m of water column (about half of the most severe previously mentioned). For a blocked regulating gate at 100% opening, the maximum observed pressure fluctuation amplitude is about 4 to 5 m of water column (1/4 to 1/5 of the most severe situation).

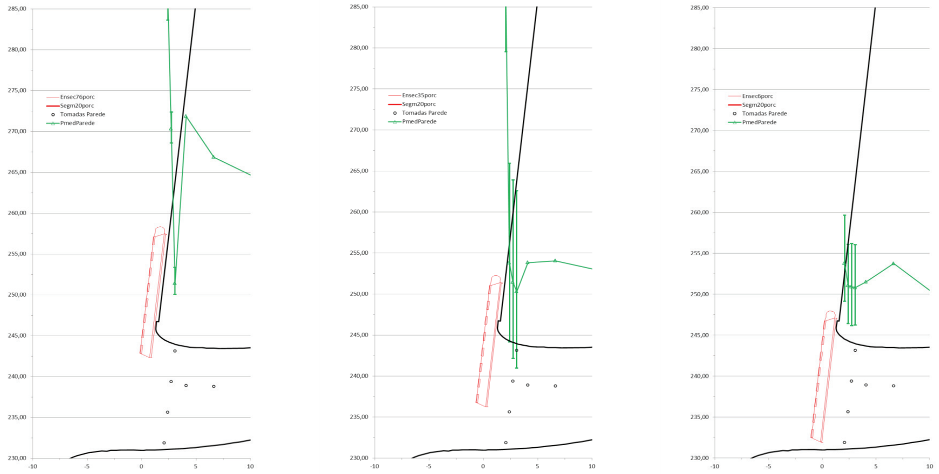

**Figure 9** : Amplitude of dynamic pressure fluctuations on the orifice side walls immediately downstream the stoplog (regulating gate 100%,60% and 20%).

The dissipation of hydraulic energy can be described by the spectra of recorded pressure fluctuations for each blocked regulating gate scenario. The spectra for the cases of 100%, 60% and 20% of regulating gate opening position are shown in the graphs in Figure 10, in which, for a comparative reading of the graphs, it is remarked that the vertical scales are distinct. It becomes evident that the situation with the highest energy associated to pressure fluctuations is the one corresponding to the regulating gate at 60% opening, which is one order of magnitude higher than for the situations of with 20% and 100%. Also, for the 60% opening, an energy concentration was detected at frequencies between 0.6 Hz and 0.7 Hz, which was not observed in the other scenarios. However, for all scenarios, most fluctuating pressure energy lies in the range below 0,1 Hz.

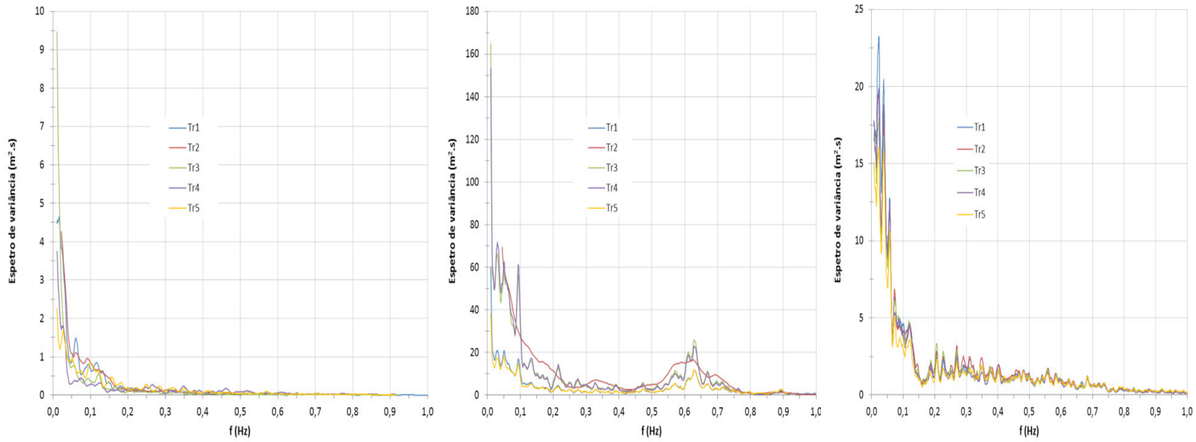

**Figure 10** : Pressure fluctuations Spectra. Scenarios with regulating gate at 100%, 60% and 20% opening.

### 2.3.2 *Unsteady state simulations – downpull assessment*

Figure 11 shows the five experimental stoplog downpull curves assuming the blockage of the regulating gate at 20%, 40%, 60%, 80% and 100% opening positions. The curves evidence that the high flow velocity near the stoplog bottom lip produces a very significant suction effect. For example, for an eventual blockage of the regulating gate in fully open position, the stoplog is subject to downpull force even before its own lower lip passes below the orifice sill beam (A zone in the graph in Figure 11).

Another important result from model tests and measurements is that the stoplog presents a closing trend throughout its course, with emphasis to the final phase of the closure. This is an essential aspect in order to guarantee that the gate can descend all the way down to full closure relying only on its own weight and downpull action.

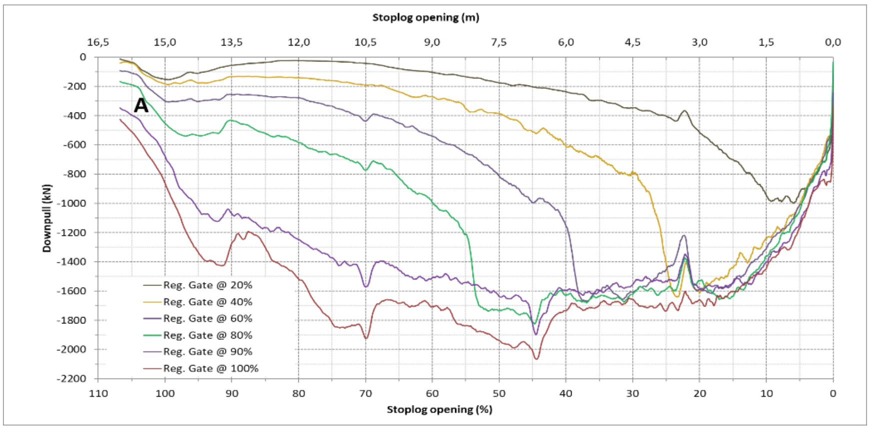

**Figure 11** . Experimental downpull curves for each regulating gate blockage scenario

## 2.4 Main results from the hydraulic models

The hydraulic model studies led to the following conclusions:

- As the stoplog descends, the average pressures within the orifice in the zones above the stoplog lower lip are much lower than those observed in normal operation, i.e., with flow being controlled exclusively by the regulating gate;
- There is a range of stoplog positions for which considerable disturbed pulsatory-type flow is observed in the orifice, between the stoplog and the regulating gate;
- Blocked positions of the regulating gate between 40% to 60% generate the most pronounced pressure fluctuation conditions inside the mid-level orifice spillway, the maximum amplitude of the observed fluctuations having reached 26% of the upstream total head of 85 m;

- Blocked positions of the regulating gate with openings below 20% lead to much less intense pressure fluctuations in the orifice;
- Downpull on the stoplog under full head is oriented downwards along the entire path, the maximum value of approximately 1,900 kN being reached when airflow through the air vents begins to be observed (maximum depression inside the orifice), and decaying progressively for stoplog openings below 20% to a value of approximately 600 kN when it fully closes.

## 3. RADIAL GATES REHABILITATION AND INSTRUMENTATION

During the rehabilitation work, through a dimensional survey campaign, considerable misalignment was found between the gate structure and the lateral sealing and roller stainless steel fixed parts. In most of the gates, strong contact of roller guides was noticed (Fig. 12, left side). Due to the close gaps (theoretically 5mm) within the gate leaf and fixed parts and the stresses this contact could cause, it was concluded that these misalignments would interfere with the gate's movement during discharge operations. The following project, concerning safety issues, aimed at finding the misalignments causes and their magnitude. Prior to its installation in all mid-level spillways, a gate instrumentation system was designed and installed in two of eight the radial gates.

### 3.1 Materials and methods

The gate instrumentation system is mainly formed by (i) the measurement sensors, including video cameras, pressure gauges and unidirectional and rectangular rosettes strain gauges; (ii) cabling system for power supply and data transfer; (iii) signal conditioners junction boxes and electrical boards with all the necessary equipment and (iv) software program developed to present and store real time results. As the most important and innovative part of the work done, one can refer the installed strain gauges. Per gate, twelve unidirectional (U-type) and eight rectangular rosettes (R-type) were installed in the following locations:

(a) One U-type on each guiding roller support, for measuring the force applied by the rollers on the lateral fixed part;

(b) Four U-type (in pairs) on the web of each of the arms upper beam;

(c) Two R-type on the external side of each support of the trunnions (Fig. 12, right side).

**Figure 12** : Roller marks on lateral upper fixed parts (left) and rosettes glued to a trunnion support (right).

As the system was designed for a wider period, the difficult of access (only by scaffolding erection) to some locations for maintenance and repair had to be considered when selecting the quantities needed – therefore two strain gauges were installed in similar spots.

The main constraints to the system design were:

- Access to most intervention areas was only possible by erecting scaffolding systems;
- The impossibility of using the spillway during the intervention period;
- Tough atmospheric conditions, with air temperatures of around 36ºC (locally increased by solar heating of the downstream face concrete and steel parts) and high relative humidity (60-80%), that reach higher values during spillway operation.

Considering that last point, significant effort to the protection system was given. In the arms, the gauges were even installed inside bottom-opened aluminum junction boxes.

### 3.2 Results

After the installation of the instrumentation system on each gate, a set of typical gate movement operations was conducted to test the system behavior (Fig. 13). It consisted in recording values during:

- Bagging of mid-level orifice by a small opening of radial gate with upstream stoplog installed;
- Two complete opening and closure of the radial gate in dry conditions;
- Water filling of mid-level orifice by a small opening of the three upper elements of the stoplog;
- Two complete opening and closure of the radial gate in wet conditions.

Perfect consistency between the expected tests values and the test results was found. The second equivalent tests led to very similar force and stress values. The similar results between the first and the second test confirmed the correct installation of the system. In both gates significant efforts in the rollers were measured and its magnitude was in line with the visually observed marks on lateral fixed parts. In the presented case, it was even possible to perfectly match the high effort zones with the dimensional survey conducted a couple of years before.

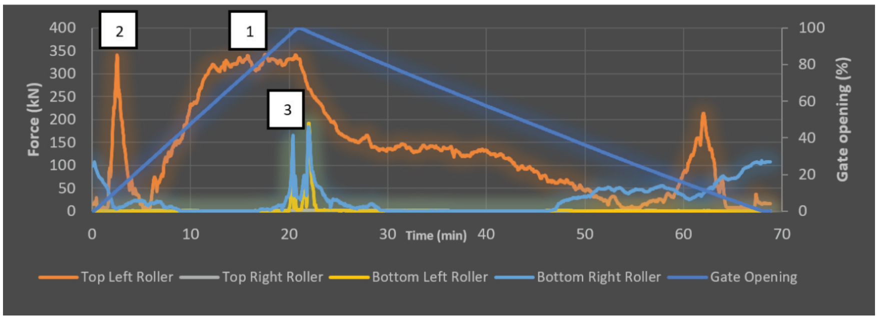

**Figure 13** : Gate No.2 - Wet Test - Applied force on the rollers.

In the gate's arms no significant defects were found except for the moment when upper left roller passed through zone 2 in Figure 14, creating a relative tensile stress in the gauges facing left side and relative compression stress in the gauges on the opposite side. In most of the trunnions strain gauge rosettes no defects were found, mainly when compared to the effort imposed by the hydrostatic pressure. Presently, this instrumentation system is in full use by HCB.

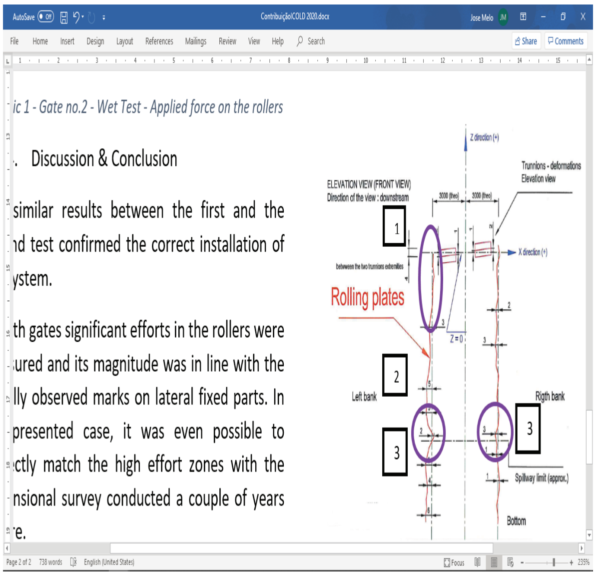

*ic 1 - Gate no.2 - Wet Test - Applied force on the rollers*

. Discussion & Conclusion

similar results between the first and the
nd test confirmed the correct installation of
ystem.

th gates significant efforts in the rollers were
ured and its magnitude was in line with the
lly observed marks on lateral fixed parts. In
presented case, it was even possible to
ctly match the high effort zones with the
nsional survey conducted a couple of years
e.

**Figure 14** : Existing dimensional survey with relevant zones.

## 4. DISCUSSION & CONCLUSION

Signs of dam deformation due to expansive reactions of concrete are affecting the mid-level orifices' geometry, namely the rectangular cross-sections where the regulating gates operate. This situation led the dam owner HCB to take multiple measures to correct, control and mitigate it. Particularly noteworthy measures are:

- The implemented instrumentation of the eight mid-level spillway regulating gates, allowing a continuous monitoring of the efforts during operation;
- The hydraulic studies of the stoplog operation under full head, which made it possible to define operation recommendations, which basically identified a safe range for stoplog operation when the regulating gate is either at fully open position or for openings smaller than 20%.

## ACKNOWLEDGMENTS

The authors would like to thank HCB for granting the approval to write this paper and to University of Lisbon, namely to Prof. Vitor Sousa, for the support provided in the numerical modelling.

## REFERENCES

Botha, A.J.; Carvalho, A.C.; Chipuazo, J.; Carvalho, E.; Boulat, L.; Hensi, D. & Chatron, C. 2016. Practical lessons learnt from the rehabilitation of spillway gates at Cahora Bassa Dam. *International Symposium on Appropriate technology to ensure proper Development, Operation and Maintenance of Dams in Developing Countries Johannesburg, South Africa, 18 May* (ISBN 978-0-620-71042-8).

Ferziger, J. & Peric, M. 2002. Computational methods for fluid dynamics, *Springer*.

Hirt, C.W. & Nichols, B.D. 1981. Volume of Fluid (VOF) method for the dynamics of free boundaries, *Journal of Computational Physics* 39, 1, 201-225.

Launder, B.E. & Spalding, D.B. 1972. Lectures in Mathematical Models of Turbulence, *Academic Press.*

LNEC, 2019. Cahora Bassa Dam. Hydraulic model study of the stoplog operation in the mid-level spilllway under full flow conditions. *LNEC - Proc. 0605/121/20574. Relatório 13/2019. DHA/NRE* (in Portuguese).

Pope, S.B. 2000. Turbulent Flows, *Cambridge University Press*, UK.

UA 2018. Numerical study on gate maneuvers in orifice spillway flows. *Department of Civil Engineering, University of Aveiro, December* (in Portuguese).